Multi-Objective Sizing of Solar-Wind-Hydro Hybrid Power System with Doubled Energy Storages under Optimal Coordinated Operation Strategy

Su Guo, Aynur Kurban, Yi He, Feng Wu, Huanjin Pei, and Guotao Song

***Abstract*—More and more attention has been paid to the high penetration of renewable energy in recent years. The randomness and intermittency of solar and wind energy make it an inevitable trend that renewables are coupled with energy storage technologies. Pumped Hydro Storage (PHS) is the most widely-used storage form in the power grid but the capacity is limited by geographic condition. The Concentrated Solar Power (CSP) plant with Thermal Energy Storage (TES) system can realize friendly grid connection and effective peak shaving. Therefore, this paper proposes a Solar-Wind-Hydro hybrid power system with PHS-TES double energy storages, and investigates the optimal coordinated operation strategy and multi-objective sizing. The optimal sizing problem which considers the minimum Levelized Cost of Energy (LCOE) and Loss of Power Supply Probability (LPSP) as objectives is solved by multi-objective particle swarm optimization. Moreover, the seasonal uncertainties of renewables are considered by scenario-based analysis using K-means clustering. Finally, the case study reveals the effectiveness of the coordinated operation strategy and double energy storages from the perspectives of economy and reliability. The comparisons of optimal sizing results show that the PV-Wind-CSP-PHS system decreases the LCOE by 19.1% compared to PV-Wind-CSP system under the same LPSP, and reduces the LPSP compared to PV-Wind-PHS system with limited reservoir capacity, which indicates that the proposed system with double energy storages has better economy and reliability performance compared to either single storage.**

***Index Terms*—Solar-Wind-Hydro, Hybrid renewable energy system, Double energy storages, Coordinated operation strategy, Multi-objective sizing optimization.**

I. Introduction

At present, two 10 million kilowatt level renewable energy demonstration bases are under construction in Hainan and Haixi, Qinghai, China [1]. The hybrid renewable energy system (HRES) based on the complementary characteristics of renewable energy has attracted more attention. HRES can coordinate various renewable energy power generation forms to achieve complementary power generation, and reduce the adverse impact on the grid [2]. Sizing optimization is the key to the design of HRES and the basis of optimal scheduling. By optimizing the capacity ratio of all kinds of renewable energy, the reliable and stable power supply of the whole system can be realized. Furthermore, the system economy and energy utilization can be improved.

A. Literature review

The existing research works on HRES mainly focus on wind-photovoltaic (PV) power generation system [3-5], photovoltaic-concentrated solar power (PV-CSP) power generation system [6-8], PV-wind-hydropower generation system [9], PV-wind-storage (battery) power generation system [10-12], etc. Energy storage system is an important part of HRES, which can improve energy utilization rate and suppress power fluctuation. PV and wind power, which are greatly affected by the random and intermittent resources, need to be equipped with large capacity energy storage devices [13]. Annette Evans et al. [14] studied and compared multiple energy storage forms of renewable energy. Among them, PHS is the most mature storage system with lower investment risk and power generation cost, battery storage (BS) system is characterized by fast response, high energy density but high cost and short cycle life, TES system has low cost and large capacity, but the conversion loss from heat to electricity is inevitable. A review of sizing optimization of the HRES according to different energy storage forms is shown as follows.

PHS is a comparatively ideal energy storage form because of its low cost and mature technology. Nyeche. et al. [15] proposed a clean, reliable and affordable hybrid wind and solar power system with a PHS. Genetic algorithm was adopted to optimize the PHS capacity to minimize the difference between energy demand and supply. Wu et al. [16] established a capacity optimization model aiming at minimizing life cycle cost and considering the constraints of power supply reliability and water balance of upper reservoir. The results demonstrated that the PV-wind-PHS system can supply reliable and stable power when operated off-grid and on-grid. Anagnostopoulos et al [17] proposed a hybrid generation model of wind power and pumped storage energy for reducing wind curtailment. A numerical method was used to optimize the size of each part of the PHS station. The optimization results showed that the model improves the utilization ratio and cost-effectiveness of wind energy. Xiao et al [18] investigated the power supply

Manuscript received June 30, 2020. This work was supported by the National Key Research and Development Program of China 2018YFE0128500 and the Fundamental Research Funds for the Central Universities of China under Grant B210202069.

S. Guo (corresponding author, e-mail: guosu81@126.com), A. Kurban (co-first author, e-mail: 2223212383@qq.com) and Yi, Wu, Pei, Song are with the School of Energy and Electricity, Hohai University in Nanjing, CO 211100 China.

DOI: 10.17775/CSEEJPES.2021.00190

reliability and investment cost of PV-wind-PHS hybrid energy system considering the solar and wind curtailment. The results showed that, compared with PV-PHS system and wind-PHS system, the PV-wind-PHS hybrid power system is the most cost-effective and reliable combination. However, none of the above studies considered the geographical constraints of PHS station which is inevitable in actual construction.

Batteries, which are characterized by fast response, relatively mature technologies and no natural conditions limit, are widely applied in HRES. Ekran et al [5] applied battery storage in a PV-wind hybrid power system and optimized the capacity with response surface methodology. Liu et al [19] improved the utilization and overall energy efficiency of wind power by integrating with lithium battery. Wang et al. [20] studied an optimal capacity configuration model considering the operation constraints of battery system and wind power characteristics. The responsive sodium-sulfur batteries were used as energy storage units in this wind-storage hybrid system. The results indicated that the proposed model has better economic performance and stable power output. Liu [21] proposed an optimization model aiming at the minimum total system cost, loss of power supply and the minimum surplus of power supply based on the battery charge and discharge constraints, the wind-solar complementary characteristics constraints and the number of power supply constraints. However, BS construction is limited from December 2019 according to the policy of State Grid Corporation of China [22], in addition, the economy of BS is not as good as TES [23, 24].

TES system is relatively cheap and easy for large-scale construction. The CSP plant coupled with TES is already available in the market [8]. Starke et al. [8] investigated the capacity optimization of a standalone CSP-PV hybrid system, which considered LCOE and capacity factor as objectives and optimized with NSGA-Ⅱ algorithm. The results demonstrated that CSP-PV hybrid system has higher capacity factor than single PV plant and lower LCOE than single CSP plant. Yang et al. [25] validated the feasibility and reliability of electric heater in wind-CSP system, which can convert the excess electricity into thermal energy stored in TES for supplying the shortage. Zhai et al. [24] analyzed the economic performances of a PV-CSP hybrid power system which applied low-cost TES as storage unit rather than expensive batteries. The results showed that the economy of the system is better than conventional PV-CSP system. However, the TES generates electricity by power block based on steam Rankine cycle and the conversion efficiency from heat to electricity is about 40% [23], which will result in much energy conversion losses. Nevertheless, the conversion efficiency of PHS is about 80% [26]. Therefore, developing TES-PHS hybrid storage is helpful to improve the system overall efficiency.

There is only one form of energy storage in the all above HRES, whereas combinations of hybrid storage are likely to be more cost-effective than a single storage technology [27]. Different energy storage has different characteristic discharge durations. Alaaeldin et al. [28] studied a double storage system applied in HRES, in which batteries are served as the backup energy storage of PHS. Adriana et al. [29] proposed a PV-CSP hybrid system with hybrid BS-TES storage units, in which TES utilization hours and the battery size were studied and the performance of the power plant was analyzed according to the capacity factor and LCOE. The result showed that the capacity factor of PV-CSP hybrid power system was increased by 5-6% compared to the PV-BS plant with the same LCOE. Yu et al. [30] optimized the capacity of battery and super capacitor based on the complementary characteristics with genetic algorithm, which considered the minimum system cost as the optimization objective. The results showed that the wind-solar hybrid power system with hybrid energy storage could better satisfy the scheduling requirements. Obviously, it is very meaningful to use multiple energy storage in HRES.

Uncertainty analysis of the input variables is necessary to simulate the actual HRES operation. Zeynali et al [31] studied two-stage stochastic programming to handle the load demand, price, and solar irradiation uncertainties in a smart home application. Wang et al [32] solved the uncertainty problem with a Scenario-dominance based NSGA-Ⅱ method. However, there were only two scenarios considered in this research. In terms of our current literature research, few works took the seasonal effect on solar, wind resources into account in uncertainty analysis.

B. Aims and contributions

According to the above analysis, this study proposes a new solar-wind-hydro hybrid power system with thermal energy storage and pumped hydro storage (PV-wind-CSP-PHS). The contributions are as follows:

(1) The coordinated operation strategy of double energy storages is proposed, in which the coordinated operation strategy is optimized by considering the charging and discharging priority of TES and PHS.

(2) The multi-objective robust sizing optimization of the proposed system based on optimal coordinated operation strategy is investigated while the seasonal uncertainties of renewables are considered in system operation based on scenario-based analysis using K-means clustering.

(3) The effectiveness of double energy storages is validated by comparing with either single storage, which indicates that the proposed system with double energy storages has better economy and reliability performance.

The remaining of this paper is organized as follows: The model of PV-wind-CSP-PHS hybrid power system and uncertainty analysis are introduced in Section 2. The sizing optimization model is established to minimize the LCOE and LPSP, and optimization process is displayed in Section 3. Section 4 and Section 5 are analysis and conclusion respectively.

II. MODELING OF HYBRID POWER SYSTEM

A. Structure model

In order to provide continuous, stable and high-quality clean energy for the power grid, this paper proposes a PV-wind-CSP-PHS system. The simplified structure of the hybrid power system is shown in Fig. 1.

This system contains wind power subsystem, PV power

subsystem, CSP subsystem, PHS subsystem and electric heater. PV and wind power generation are mainly used to meet the load demand while CSP plant and PHS station play a regulating role. Specifically, when the supply exceeds the load demand, the surplus power is absorbed by the hybrid storage. Otherwise, the deficiency power is supplied by the double storages.

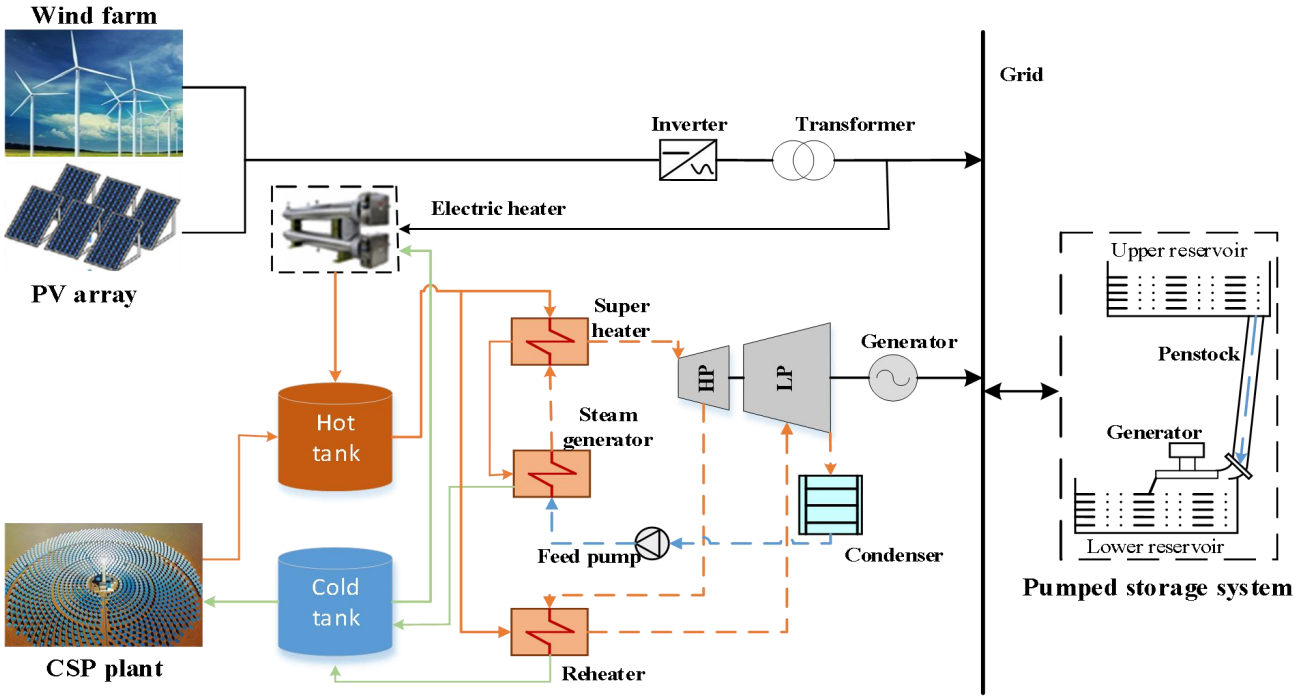

Fig. 1. PV-wind-CSP-PHS hybrid power system

B. Uncertainty analysis of solar and wind resources

A stochastic scenario-based analysis using K-means clustering algorithm is applied to analyze the uncertainties of renewable energy resources. K-means clustering algorithm iteratively classifies the scenarios into different typical clusters to minimize the square error function [33]. In this paper, the Squared Euclidean distance is adopted to generate typical scenarios, defined as follows:

$$d\left(x,c_k\right)=\sum_{k=1}^{K}\sum_{x\in C_k}\left\|x-c_k\right\|^2 \tag{1}$$

where K is the number of clusters, x is the scenarios, and c_k is the center of k^{th} cluster denoted by C_k .

Due to the significant impact of seasons on solar and wind energy resources, the scenario analysis method is specifically investigated for different seasons. The specific procedures of K-means clustering are as follows:

(1) The daily solar radiation and wind speed are taken as a scenario. Divide the 365 scenarios of a year into four parts according to seasons.

(2) Randomly select K initial cluster centers from all scenarios in each season as the typical scenarios.

(3) Minimize the Euclidean distance from each scenario to its cluster center.

(4) The cluster centers are recalculated until the Euclidean distance from each scenario to its closest cluster center is converged.

(5) The probability of typical scenario is the rate between the number of each typical scenario group and all scenarios.

A series of typical scenarios and their occurrence probability are obtained based on above procedures according to the historical data of the study area. In Fig.2, the thin lines represent the whole scenarios for each season and the thick lines of color represent the typical scenarios of solar radiation and wind speed.

Stochastic curves of resource in one year are obtained by selecting 365 times randomly based on the above typical scenarios and corresponding probability. The curves in N years are obtained to prepare data for the application of robust optimization.

C. Mathematical model

The following is the mathematical model of each subsystem.

According to the rated power of the wind turbine and wind speed uncertain parameters, the output power of the wind turbine is calculated by following formula [21, 34]:

$$P_{\text{wind}}=\begin{cases}0 & v<v_i \text{ or } v>v_o\\ f(v) & v_i\le v\le v_{\text{r}}\\ P_{\text{r}} & v_{\text{r}}\le v\le v_o\end{cases} \tag{2}$$

$$f(v)=\frac{v^3-v_i^3}{v_{\text{r}}^3-v_i^3}P_{\text{r}} \tag{3}$$

where P_{wind} is the wind turbine output power, kW; P_{r} is the rated power of wind turbine, kW; v_i , v_o are the cut−in, cut−out speed respectively, m/s; v_{r} is the wind turbine rated speed, m/s;

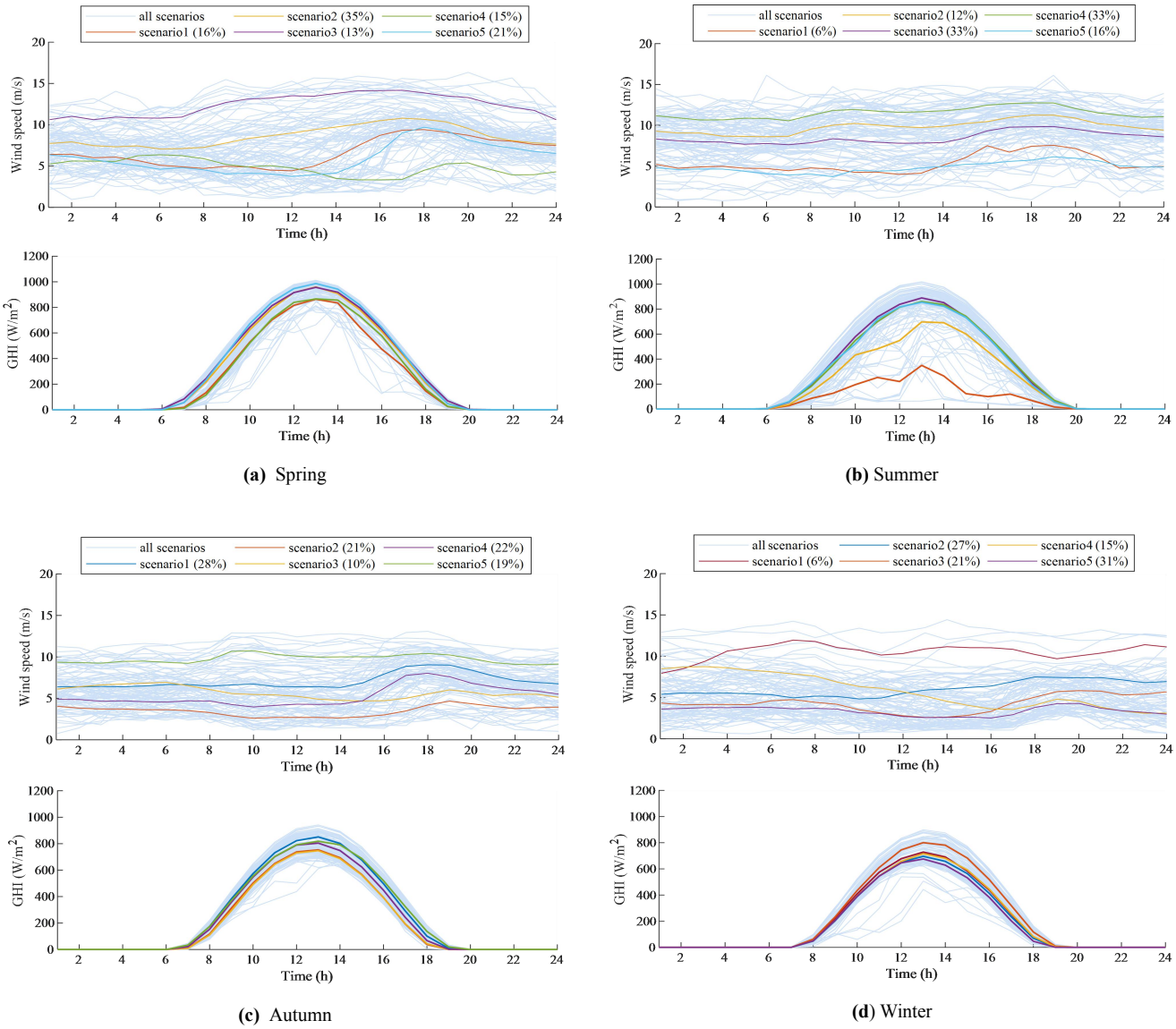

Fig. 2. Typical scenarios of renewable energy and their occurrence probability

v is the predicted wind speed, m/s.

The output of PV is mainly related to solar radiation and temperature. The simplified model of PV, which considering the uncertainty of solar radiation, is shown as follows [34, 35]:

$$P_{\mathrm{pv}} = P_{\mathrm{STC}} \cdot (1 + \beta(T - T_{\mathrm{STC}}))I / I_{\mathrm{STC}} \tag{4}$$

$$T = T_{\mathrm{amb}} + 30I / I_{\mathrm{STC}} \tag{5}$$

where P_{pv} is the output power of photovoltaic cells, kW; P_{STC} is the maximum output power under the standard test conditions (STC), kW; I_{STC} is the STC solar irradiance, 1000W/m^2; I is the predicted solar irradiance, W/m^2; β is the temperature coefficient, taken as -0.47%/K; T is the surface operation temperature of photovoltaic cells, ℃; T_{STC} is the STC temperature, 25 ℃; T_{amb} is the ambient temperature, ℃.

The output power of the CSP plant is calculated by the minute-scale performance evaluation software independently developed by the authors' research group. The main mathematical models are as follows.

(1) Heliostat field model:

$$q_{\mathrm{h}} = S_{\mathrm{area}} \cdot DNI \cdot \eta_{\mathrm{l}} \tag{6}$$

$$\eta_{\mathrm{l}} = \eta_{\mathrm{foc}} \cdot \eta_{\mathrm{ref}} \cdot \eta_{\mathrm{hel}} \cdot \eta_{\mathrm{wind}} \tag{7}$$

where S_{area} is the effective area of heliostats, kW; DNI is the direct normal irradiance, kW/m^2; η_{l} is the heliostat field efficiency; η_{foc} is the focusing efficiency; η_{ref} is the mirror reflection efficiency; η_{hel} is the optical efficiency; η_{wind} is the wind influence.

(2) Receiver model

Energy balance equation outside tube:

$$q_{\mathrm{in}} = q_{\mathrm{inc}} - \left(q_{\mathrm{ref}} + q_{\mathrm{rad}} + q_{\mathrm{conv}}\right) \tag{8}$$

$$q_{\mathrm{inc}}(x) = D_{\mathrm{tube}} \cdot n_t \int_{x_0}^{x_0+\Delta x} P''_{\mathrm{field}}(x)\,dx \tag{9}$$

$$q_{\mathrm{ref}}(x) = (1-\alpha) D_{\mathrm{tube}} \cdot n_t \int_{x_0}^{x_0+\Delta x} P''_{\mathrm{field}}(x)\,dx \tag{10}$$

$$q_{\mathrm{rad}}(x)=\sigma\varepsilon\pi\cdot\frac{D_{\mathrm{tube}}}{2}\cdot F_{t,s}\cdot n_t\int_{x_0}^{x_0+\Delta x}\left[T_{\mathrm{s}}^4(x)-T_{\mathrm{amb}}^4\right]dx \tag{11}$$

$$q_{\mathrm{conv}}(x)=h_{\mathrm{m}}\cdot D_{\mathrm{tube}}\cdot n_t\int_{x_0}^{x_0+\Delta x}\left[T_{\mathrm{s}}^4(x)-T_{\mathrm{amb}}^4\right]dx \tag{12}$$

where q_{in} is the inlet heat of the collector; q_{inc} is the incident radiation; x is the thickness of tube; q_{ref} is the tube surface reflection; q_{rad} is the radiation heat transfer; q_{conv} is the external convection heat transfer. D_{tube} is the tube diameter; n_t is number of tubes per panel; P''_{field} is the dense distribution of energy flow; $1-\alpha$ is the reflectivity; ε is the emissivity and σ is the Stefan-Boltzmann constant; $F_{t,s}$ is the angle factor; $T_{\mathrm{s}}(x)$ and T_{amb} are the external surface temperature and ambient temperature of heat receiver; h_{m} is the mixed convection heat transfer coefficient.

Heat transfer equation in tube:

$$q_{\mathrm{in}}=\left(T_{\mathrm{s}}-T_{\mathrm{HTF}}\right)\cdot\frac{1}{R_{\mathrm{cond}}+R_{\mathrm{conv}}} \tag{13}$$

where T_{HTF} is the average temperature of transfer fluid; R_{cond} and R_{conv} are the heat loss of heat conduction and convection between the inner wall of the tube and the transfer fluid.

(3) TES model

The TES system uses the cold tank and hot tank storage mode with molten salt heat transfer fluid. The state model of the thermal storage system is shown as follows:

$$\frac{dM}{dt}=m_i-m_0 \tag{14}$$

$$C_{\mathrm{p}}\frac{d(MT)}{dt}=m_iC_{\mathrm{p}}T_{\mathrm{h}}-m_0C_{\mathrm{p}}T-(UA)_t\left(T-T_{\mathrm{amb}}\right) \tag{15}$$

where M is the instantaneous mass of transfer fluid in tank; t is the temperature of transfer fluid; m_i and m_0 are the net inlet flow rate and net outlet flow rate; C_{p} is the specific heat of transfer fluid; T, T_{h} are the instantaneous temperature of transfer fluid and inlet transfer fluid temperature; $(UA)_t$ is the total heat loss coefficient of tank.

(4) Turbine model

In this part, a typical turbine unit model with eight stage extraction is described. On startup, the parameters such as main steam flow, temperature and pressure are calculated according to the turbine starting curve under different starting conditions. The turbine start-up operation stage is decided according to the inlet temperature.

The transformation models from electricity to water potential energy of PHS system [16, 36]:

$$W_i(t)=\frac{\eta_{\mathrm{pump}}E_{\mathrm{p}}(t)}{\rho gh} \tag{16}$$

$$\eta_{\mathrm{pump}}=\eta_{\mathrm{p}}\cdot\eta_{\mathrm{m}}\cdot\eta_{\mathrm{pipe}} \tag{17}$$

where $W_i(t)$ is the pumping capacity of water pump in t period, m^3; $E_{\mathrm{p}}(t)$ is the power consumption in t period, kWh; ρ is the water density, 1000kg / m^3; g is the gravity coefficient, 9.81m/s^2; h is the mean head, m; η_{p}, η_{m}, η_{pipe} are the efficiencies of pump, motor, and pipe and taken as 0.92, 0.95, 0.95 respectively.

The transformation model from water potential energy to electricity:

$$E_{\mathrm{g}}(t)=\eta_{gen}\cdot\rho gh\cdot W_o(t) \tag{18}$$

$$\eta_{gen}=\eta_{\mathrm{tr}}\cdot\eta_{\mathrm{gr}}\cdot\eta_{\mathrm{pipe}} \tag{19}$$

where $E_{\mathrm{g}}(t)$ is the output power of hydraulic turbine in t period, kWh; $W_o(t)$ is the water consumption for power generation in t period, m^3; η_{tr}, η_{gr}, and η_{pipe} are the efficiencies of turbine, generator, and pipe and taken as 0.89, 0.95, 0.95 respectively.

III. Capacity Optimization of Hybrid Power System

A. Objective function

The optimization objectives of this paper are minimizing Levelized Cost of Energy (LCOE) and Loss of Power Supply Probability (LPSP).

1) LCOE

$$LCOE=\frac{IC_{\mathrm{w}}+IC_{\mathrm{pv}}+IC_{\mathrm{csp}}+IC_{\mathrm{phs}}+\sum_{n_1=1}^{N}\frac{AC_{\mathrm{w}}+AC_{\mathrm{pv}}+AC_{\mathrm{csp}}+AC_{\mathrm{phs}}}{(1+i)^{n_1}}}{\sum_{n_1=1}^{N}\frac{E_{\mathrm{sys}}(1-d_{\mathrm{sys}})^{n_1}}{(1+i)^{n_1}}} \tag{20}$$

where IC_{w}, IC_{pv}, IC_{csp} and IC_{phs} are the initial cost of wind, PV, CSP and PHS system respectively, \$/kW; AC_{w}, AC_{pv}, AC_{csp} and AC_{phs} are the operation and maintenance cost of above system respectively, \$/kW; E_{svs} is the first-year power generation of the system, kWh; d_{svs} is the degradation rate; i is the discount rate; N is the life cycle [23, 24].

2) LPSP

In this PV-wind-CSP-PHS hybrid power system, PV and wind are responsible for meeting the load demand of the system. When wind and photovoltaic power fails to meet the load demand and PHS system and TES system cannot either supply the deficient electricity, the system load cannot be satisfied. Therefore, the variable of LPSP is introduced in this paper. LPSP indicates that the proportion of the unmet power demand to the total power demand in a year, which is expressed as follows [21]:

$$LPSP=\frac{\sum_{t=1}^{m_l}\left|P_{\mathrm{l}}(t)-P_{\mathrm{w}}(t)-P_{\mathrm{pv}}(t)-P_{\mathrm{csp}}(t)-P_{\mathrm{phs}}(t)\right|}{\sum_{t=1}^{8760}\left|P_{\mathrm{l}}(t)\right|} \tag{21}$$

where $P_{\mathrm{l}}(t)$ is the power load at the sampling point t, kW; $P_{\mathrm{w}}(t)$, $P_{\mathrm{pv}}(t)$, $P_{\mathrm{csp}}(t)$ and $P_{\mathrm{phs}}(t)$ are the output power of wind, PV, CSP and PHS system at the sampling point t, kW; m_l is the number of unmet load sampling points.

3) Objective function

In the system with good robustness, the variables will ensure achieving the optimal solution under the worst case [37]. In order to improve the robustness of simulation results, the maximum objective functions value of stochastic data in N years is adopted in this paper. The optimization objective function is as follows:

$$\begin{cases}\min\max\limits_{j\in N}LCOE_j(\xi,x)\\ \min\max\limits_{j\in N}LPSP_j(\xi,x)\\ x=(C_{\mathrm{W}},C_{\mathrm{PV}},C_{\mathrm{CSP}},C_{\mathrm{PHS}})\end{cases} \tag{22}$$

where ξ is the random vector, which represents above scenarios and corresponding probability distribution; C_{W} is the wind farm capacity; C_{PV} is the photovoltaic plant capacity,

C_{CSP} is the concentrated solar power plant capacity; C_{PHS} is the pumped hydro storage station capacity.

In the objective function, *N*-year LCOE and LPSP are obtained from the operation simulation model in part *C* Fig. 3(b). Then, the maximum value of LCOE and LPSP are found as fitness function. Finally, the MOPSO algorithm explained in part *C* Fig. 3(a) returns a set of Pareto optimal solutions. These solutions may make the system have better robustness since they were obtained considering the resource uncertainty and the worst-case scenario in the optimization process.

B. Constraints

1) Constraints of TES system

$$W_{tes}^{min} \le W_{tes}(t) \le W_{tes}^{max} \tag{23}$$

$$P_{tes}^{min} \le P_{tes}(t) \le P_{tes}^{max} \tag{24}$$

where W_{tes}^{max}, W_{tes}^{min} are the maximum and minimum storage capacity of TES system, kWh; P_{tes}^{max}, P_{tes}^{min} are the maximum and minimum output of the TES system, kW.

2) Power block constraints

The operation of power block is limited by the maximum power P_{tes}^{max} and minimum power P_{tes}^{min}, and the constraint is as follows [25]:

$$P_{t,min}^{PB} \le P_t^{PB} \le P_{t,max}^{PB} \tag{25}$$

3) Constraints of PHS system

The construction of PHS station is usually restricted by the geographical location and natural resources. Thus, this paper limits PHS system under maximum developed capacity. Constraints on storage capacity of upper reservoir (UR) is:

$$V_{min}^{UR} \le V_{UR} \le V_{max}^{UR} \tag{26}$$

where V_{min}^{UR}, V_{max}^{UR} are the minimum and maximum water storage capacity of the UR, m^3; V_{UR} is the capacity of UR, m^3.

C. Optimization

1) Optimization algorithm

A multi-objective optimization model considering minimizing LCOE and LPSP as optimization objectives is established and optimized by the MOPSO in this paper. Compared with other algorithms, the MOPSO is conducive to obtain the optimal solution of multi-objectives [38, 39]. The process of optimization algorithm is shown in Fig. 3(a).

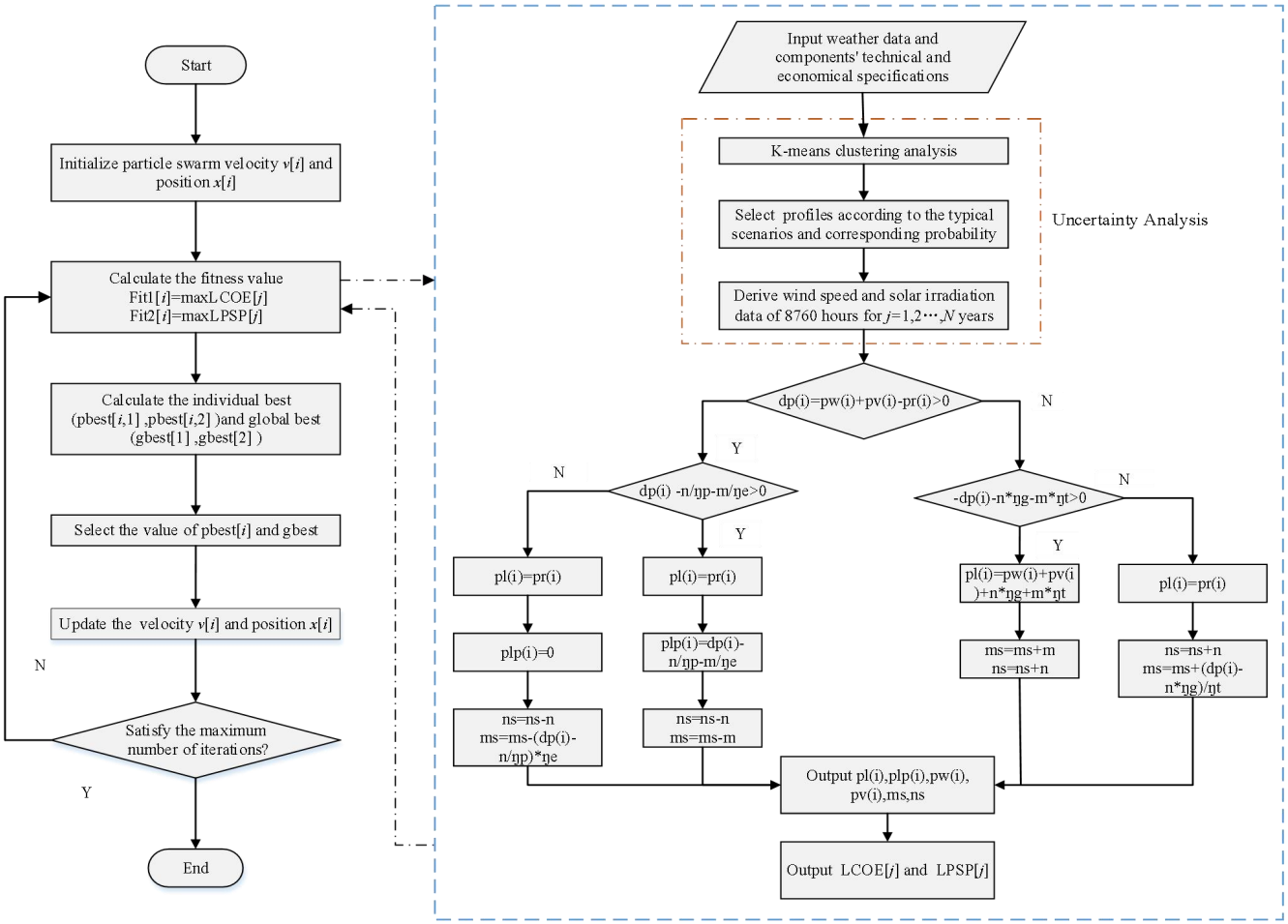

(a) The process of optimization algorithm **(b)** System operation simulation

Fig. 3. Flowchart of the proposed probabilistic simulation-based optimization approach

2) Operation strategy

The crucial objective of this paper is to investigate the optimal coordinated operation strategy of TES and PHS, thus effectively regulating the volatile power output of PV and wind power to improve the system reliability. The coordinated operation strategy is optimized by considering the charging and discharging priority of TES and PHS, which has a great influence on system performance. There are four coordinated operation strategies to be optimized according to different charging and discharging priority, which are shown as follows:

(1) Charging priority and discharging priority both for PHS;
(2) Charging priority for PHS, discharging priority for TES;
(3) Charging priority for TES, discharging priority for PHS;
(4) Charging priority and discharging priority both for TES;

The coordinated operation strategies are based on rule-based algorithms, the strategy (1) is introduced in detail and other three strategies are almost the same except for the charging and discharging priority.

Strategy (1): When the power output of PV and wind power is larger than the load demand, PHS firstly charges to absorb the excess energy and TES supplies the supplementary capacity for PHS. When the power output of PV and wind power is lower than the load demand, PHS firstly discharges to provide the deficiency and TES also supplies the supplementary energy for PHS. The simplified flow chart of strategy (1) is shown in Fig. 3(b).

In this flow chart: $\mathrm{pw}(i)$, $\mathrm{pv}(i)$, $\mathrm{pl}(i)$, $\mathrm{pr}(i)$, $\mathrm{plp}(i)$ represent the wind, PV output power, system on-grid power, real-time load, and system power consumption at period i respectively, $\mathrm{dp}(i)$ represents the difference between system power supply and load. m is the charge and discharge capacity of the TES system for period i , ms is the current capacity of the TES system, $\mathrm{ms\_max}$ represents the maximum TES capacity, and the system always meets $\mathrm{ms} \le \mathrm{ms\_max}$. n is the charge and discharge capacity of the PHS system for period i , ns is the current capacity of the PHS system, $\mathrm{ns\_max}$ represents the maximum PHS capacity and the system always meets $\mathrm{ns} \le \mathrm{ns\_max}$.

(1) $\mathrm{dp}(i) > 0$ and $\mathrm{dp}(i) - \mathrm{n}/\eta_p > 0$, it means that the output power of PV and wind are greater than the load demand, and the redundant power cannot be completely consumed by the PHS system.

(2) $\mathrm{dp}(i) > 0$ and $\mathrm{dp}(i) - \mathrm{n}/\eta_p < 0$, it means that the output power of wind and PV are greater than the load demand, and the redundant power can be completely consumed by the PHS system. So, the PHS system absorbs the excess electricity, and the TES system only needs to store the heat collected by the solar field.

(3) $\mathrm{dp}(i) < 0$ and $\mathrm{dp}(i) - \mathrm{n}/\eta_p > 0$, it means that the output power of wind and PV are less than the load demand, and the PHS station cannot fully supplement the deficient load. So, the TES system is needed to release heat for power generation.

(4) $\mathrm{dp}(i) < 0$ and $\mathrm{dp}(i) - \mathrm{n}/\eta_p < 0$, it means that the output power of wind and PV are less than the load demand, and the PHS station can fully supplement the rated load.

IV. CASE STUDY

A. Main parameters of power supplies

The main parameters of the wind turbine and PV panel are displayed in Table Ⅰ and Table Ⅱ. The main parameters of CSP plant and PHS station are shown in Table Ⅲ and Table Ⅳ.

TABLE Ⅰ.
MAIN PARAMETERS OF WIND TURBINE [28]

Parameters	Value	Unit
Model	UP77-1500	-
Rated power	1500	kW
Cut-in speed	3	m/s
Rated speed	11.5	m/s
Cut-out speed	25	m/s
Initial cost	1200	$/kW
Operation and maintenance (O&M) cost	120	$/kW

TABLE Ⅱ.
MAIN PARAMETERS OF PV PANEL [28]

Parameters	Value	Unit
PV panel model	SFM260W	-
Max power	260	W
Operating temperature	-40~80	℃
Irradiance	1000	W/m^2
Initial cost	867	$/kW
O&M cost	16	$/kW

TABLE Ⅲ.
MAIN PARAMETERS OF CSP PLANT AND TES SYSTEM [24]

	Parameters	Value	Unit
CSP plant	Heliostat field efficiency	0.60	%
	Receiver efficiency	0.5	%
	Power block efficiency	0.397	%
	Initial cost	3600	$/kW
	O&M cost	66.7	$/kW
TES system	Thermal storage capacity	10	h
	TES Initial cost	67	$/kW
	TES O&M cost	8	$/kW

TABLE Ⅳ.
MAIN PARAMETERS OF PHS STATION [36]

Parameters	Value	Unit
Rated power	10000	kW
UR capacity	684684	kWh
Pumping co-efficient	7.6	m^3/ kWh
Turbine co-efficient	0.088	kWh/m^3
Mean head	40	m
Storage duration	7	h
Initial cost	667	$/kW
O&M cost	16	$/kW

B. Output power

The solar and wind energy resource data of Karachi, Pakistan (25°04′N, 67°56′E) are used in this paper. Due to the existence of reduction coefficient, PV and wind output cannot generate at the nominal capacity. The unitized (normalized to maximum 1MW) power curve of wind farm and PV plant based on actual energy resource data in this area are displayed in Fig. 4 and Fig. 5.

The unitized power curve of CSP plant without TES system is shown in Fig. 6.

C. Algorithm validation

The Hypervolume (HV) usually is applied to evaluate the performance of multi-objective optimization algorithms, which is the volume surrounded by the non-dominated solution sets and a reference point. The larger HV value indicates the better the convergence and diversity of the algorithm [35].

TABLE Ⅴ.
COMPARISONS BETWEEN ALGORITHMS

	MOPSO	MOEA/D	NSGA-Ⅱ
HV	0.5874	0.5592	0.5936
Time (s)	68.64	128.16	146.88

In this paper, MOPSO is applied to obtain the optimal solution set and MOEA/D (Multi Objective Evolutionary Algorithm based on Decomposition) and NSGA-Ⅱ (Non-dominated Sorting Genetic Algorithm-Ⅱ) are the reference algorithm. The average HV value and computing time of MOPSO, MOEA/D and NSGA-Ⅱ for 10 runs are calculated and displayed in Table Ⅴ. It is easy to find that the HV value of MOPSO is larger than MOEA/D, which shows that MOPSO has better convergence and diversity performance than MOEA/D. The computing time of MOPSO is shorter than MOEA/D and NSGA-Ⅱ, which shows that MOPSO has faster computation efficiency. Therefore, the MOPSO algorithm has relatively better comprehensive performance.

D. Optimization results

The parameters of MOPSO algorithm are as follows: inertia weight w=0.5, learning factor c_1=1.6, c_2=2.0, search space dimension D = 4, maximum number of iterations M = 50, number of initialization particles N = 1000. The Pareto optimal solution set obtained by MOPSO algorithm is shown in Fig. 7. In order to meet the load demand, the final LPSP is bound to less than 10%. Due to the limitation of the rated capacity of each power source and the geographical location of the PHS station, the exact values of point A, B, C cannot be obtained, so the final optimization results are determined near these points. The specific values of LCOE, LPSP and the corresponding power plants' capacities are presented in Table Ⅵ. The thermal storage capacity of TES system is 10h. The rated power load of the system is 100MW.

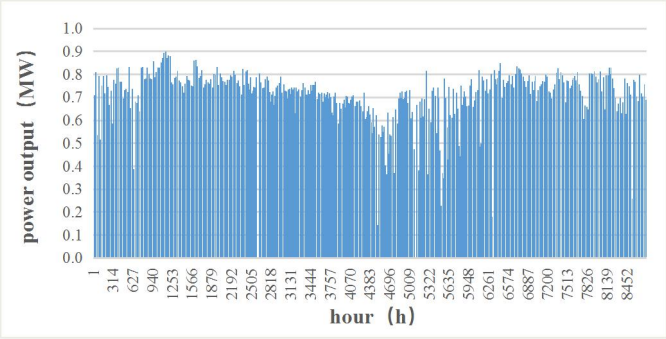

Fig. 4. The unitized power curve of PV plant

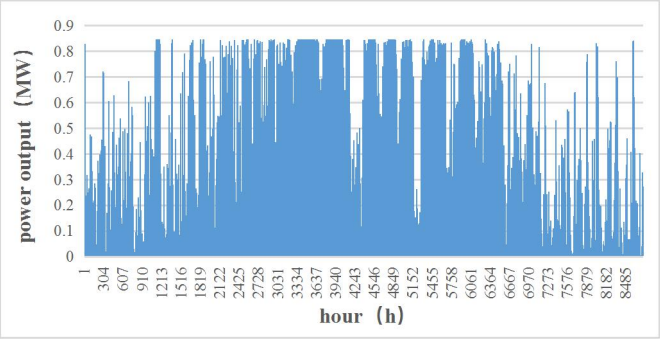

Fig. 5. The unitized power curve of wind farm

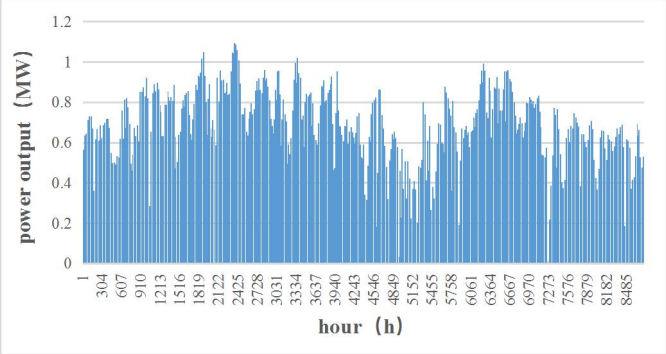

Fig. 6. The unitized power curve of CSP plant (without TES)

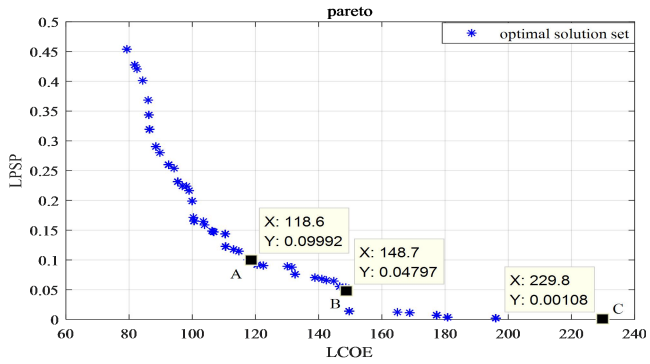

Fig. 7. Pareto optimal solution set

TABLE Ⅵ.
OPTIMIZATION RESULTS

LPSP (%)	LCOE ($/MWh)	C_W (MW)	C_{PV} (MW)	C_{CSP} (MW)	C_{PHS} (MW)
9.89	118.6	120	392.6	25	130
4.84	148.5	196.5	416	43	130
0.11	229.7	342	582.4	93	120

The power output curve of hybrid power system in a year when LPSP is 9.89% is presented in Fig. 8. It can be seen that, there are many days when the system fails to meet the load demand from January to March and from November to December. And the LPSP of these periods are 18.3% and

21.5% respectively, while the LPSP from April to October is only 5.3%. This is because the output power of wind farm from April to October is significantly higher than other times.

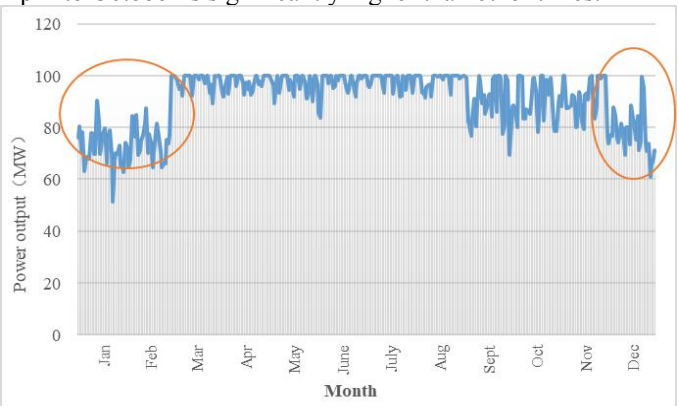

Fig. 8. Power output curve of hybrid power system

E. Comparisons and analysis of optimization results

1) Comparisons between different operation strategies

The optimization results comparison of different operation strategies under the same system capacity is shown in Table Ⅶ. It can be seen that the LCOE and LPSP of strategy (1) are lower than those of others, which indicates that Strategy (1) is the optimal coordinated operation strategy.

TABLE Ⅶ
COMPARISONS OF STRATEGIES

	Strategy (1)	**Strategy (2)**	**Strategy (3)**	**Strategy (4)**
LCOE ($/MWh)	118.6	126.0	124.5	132.1
LPSP (%)	9.89	15.18	14.11	19.07

2) Comparisons between PV-wind-PHS system and PV-wind-CSP-PHS system

Adding PHS station to the PV-wind hybrid power system can adjust the PV and wind power fluctuation effectively. However, due to the limitation of geographical location and water resources in some areas, the maximum installed capacity of PHS station is not large enough to regulate the output power. It is evident shown from Table Ⅷ that the LPSP of PV-wind-PHS system is greater than 10%, which cannot meet the specified requirements. CSP plant with TES system can realize effective peak load regulation. So, the PV-wind-CSP-PHS system, which is used as regulating power supply by CSP plant and PHS station, alleviate the above shortcomings effectively. As shown in Table Ⅷ, although the LCOE of PV-wind-CSP-PHS system is increased by 11.4 $/MWh compared to PV-wind-PHS system, its LPSP is reduced from 13.87% to 9.89%. It is obvious that PV-wind-CSP-PHS system can suppress power fluctuation better.

The representative day power output curves of PV-wind system, PV-wind-PHS system and PV-wind-CSP-PHS system are shown in Fig. 9. It can be seen that, the output power of wind PV system is less than the rated load at 1:00-9:00 and 22:00-24:00, and is greater than the rated load at 9:00-22:00. In the PV-wind-PHS system, the PHS station starts to pump water energy at 9:00, and discharges water to generate electricity at 22:00-24:00 and 1:00-4:00, so only 4:00-9:00 the load demand cannot be met. The PV-wind-CSP-PHS system includes both PHS station and CSP plant with TES system. The excess power which cannot be absorbed by the PHS station complete energy conversion by the electric heater and stored in the TES system. When the PHS station cannot continue to generate electricity, the steam turbine unit will generate electricity for supplement. Therefore, the PV-wind-CSP-PHS system can meet the load demand in most cases.

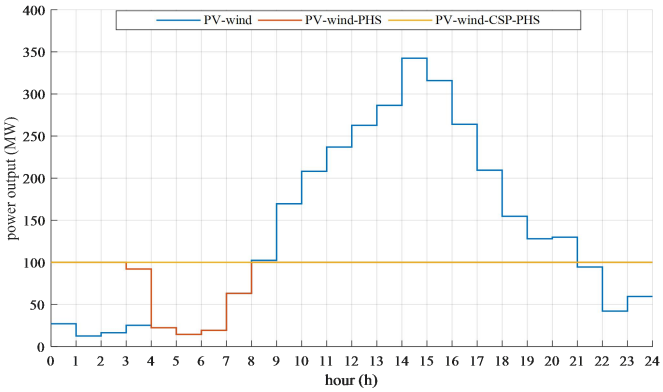

Fig. 9. Power output curve of representative day

3) Comparisons between PV-wind-CSP-PHS system and PV-wind-CSP system

In the PV-wind-CSP hybrid power system, the excess electricity of PV plant and wind farm can be converted into thermal energy by EH and absorbed by the TES system of the CSP plant. However, the construction cost of the CSP plant is high. If its installed capacity is too large, the LCOE of the system will increase rapidly. Table Ⅷ presents the comparison between the PV-wind-CSP-PHS system and the PV-wind-CSP system. Under the same LPSP, the capacity of CSP plant in PV-wind-CSP system increased from 25 MW to 89.8 MW, and the LCOE increased from 118.6 $/MWh to 146.6 $/MWh. Obviously, the PV-wind-CSP-PHS system is more cost-effective than PV-wind-CSP system.

TABLE Ⅷ.
COMPARISONS BETWEEN HYBRID POWER SYSTEMS

	C_W (MW)	C_{PV} (MW)	C_{CSP} (MW)	C_{PHS} (MW)	LCOE($/MWh)	LPSP(%)
PV-wind-PHS	120	392.6	0	130	107.2	13.87
PV-wind-CSP-PHS	120	392.6	25	130	118.6	9.89
PV-wind-CSP	120	392.6	89.8	0	146.6	9.89

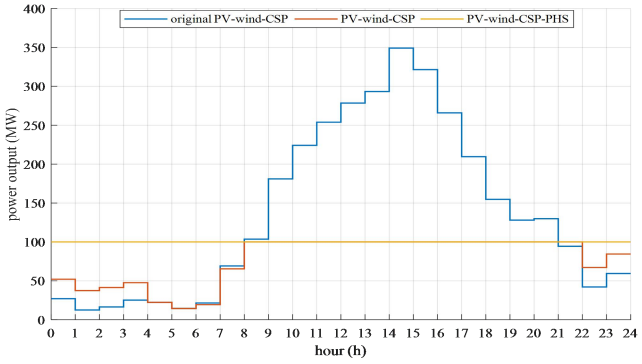

Fig. 10. Power output curve of representative day

As can be seen in Fig. 10, the power supply of PV-wind-CSP system at 1:00-5:00 and 22:00-24:00 is larger than that of conventional power generation system, but still does not meet the load demand, while the power supply of PV-wind-CSP-PHS system meet the load demand absolutely. Therefore, the PV-wind-CSP-PHS system has better power supply reliability.

V. CONCLUSION

This paper proposes solar-wind-hydro hybrid power system with thermal energy storage and pumped hydro storage (PV-wind-CSP-PHS) in view of geographical limitation of PHS station. The size optimization of hybrid power system with double energy storages under optimal coordinated operation strategy are investigated. The following conclusions can be drawn based on the results.

(1) The coordinated operation strategy of double energy storages is proposed. The comparisons of different coordinated operation strategies show that the levelized cost of energy (LCOE) and loss of power supply probability (LPSP) of operation strategy with charging and discharging priorities both for PHS are 118.6 $/MWh and 9.89% respectively and less than those of other strategies, which demonstrates that the aforementioned strategy is the optimal coordinated operation strategy.

(2) The seasonal uncertainties of solar energy and wind speed are considered based on scenario-based analysis, and the multi-objective robust size optimization is investigated to improve the robustness of the proposed system.

(3) The effectiveness of double energy storages is investigated. The optimal LPSP of PV-wind-PHS system is 13.87%, which cannot satisfy the predefined reliability constraint (LPSP < 10%). However, the introduction of CSP plant can effectively reduce LPSP to 9.89%, which indicates that the PV-wind-CSP-PHS system has better reliability performance. The LCOE of PV-wind-CSP-PHS system is decreased by 19.1% compared to PV-wind-CSP system under the same LPSP, which indicates that the proposed system is more cost-effective.

In summary, when the maximum capacity of PHS is limited, the CSP-PHS double energy storages under optimal coordinated operation strategy and installed capacity can effectively regulate renewables power to ensure better reliability and cost-effective performance.

APPENDIX A

The wind power curve of the wind turbine applied in this paper is shown in Fig. A1.

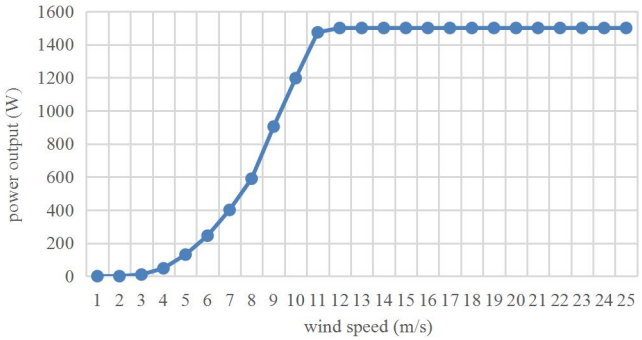

Fig. A1 The wind power curve of UP77-1500 model [40]

The I-V curve of the PV modules applied in this paper is shown in Fig. A2.

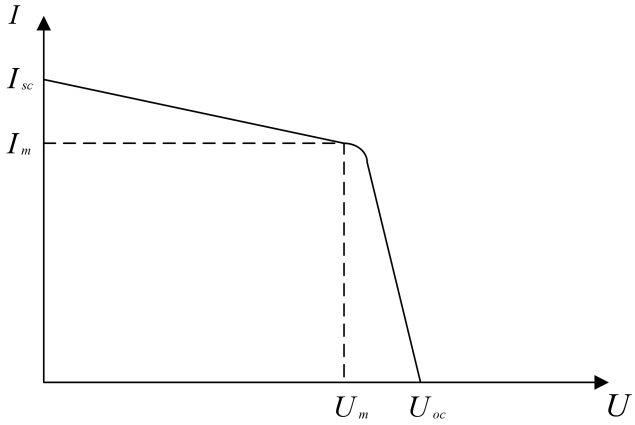

Fig. A2 The I-V curve of SFM260W model [41]

In Fig. A2, U_m is the peak voltage; U_{oc} is the open circuit voltage; I_m is the peak current; I_{sc} is the short-circuit current.

The parameters of SFM260W model are presented in Table A.

TABLE A
PARAMETERS OF SFM260W MODEL

Parameters		Parameters	
Voltage at maximum power	30.23V	Current at maximum power	8.61A
Open-circuit voltage	32.6V	Short-circuit current	9.47A
Power tolerance (positive)	+ 3 %	Power tolerance (negative)	- 3 %

REFERENCES

[1] Q. Z. Zhouqiang, "Summary and Prospect of new energy development," *Research and Approach*, vol. 40, pp.25-32,2018.

[2] W. R. Wangruichun, "Supporting effect of energy storage on renewable," *Research and Approach*, vol. 42, pp. 192-196,2014.

[3] A. K. Bouya, "Sizing methods and optimization techniques for," *RENEW SUST ENERG REV*, vol. 93, pp. 625–673, 2018.

[4] H. B. Chenbin, "Capacity optimization of hybrid energy storage unit in wind solar hybrid," *J AGR ENG RES*, vol. 27, pp. 241-245, 2011.

[5] E. O. Ekren, "Size optimization of a PV/wind hybrid energy conversion system with," *APPL ENERG*, vol. 85, pp. 1086-1101, 2008.

[6] J. A. Velázquez, "Techno-economic analysis of a hybrid PV-CSP system," *SOL ENERGY*, vol. 174, pp. 55-65, 2018.
[7] J. X. Xu, "A review on the development of photovoltaic/concentrated solar power," *SOL ENERG MAT SOL C*, vol. 161, pp. 305-327, 2017.
[8] S. A. Cardemil, "Multi-objective optimization of hybrid CSP+PV system using," *Energy*, vol. 147, pp. 490-503, 2018.
[9] Y. M. Chenshijun, "Research on capacity optimization of hydro wind power," *Hydropower Energy Science*, vol. 36, pp. 215-218, 2018.
[10] T. Y. Liwenyi, "Analysis of the influence of optimal capacity allocation of wind," *SOL ENERGY*, vol. 29, pp. 2439-2245, 2018.
[11] F. Y. Yangfan, "Research on capacity optimization of off grid," Ph.D. dissertation, Dept. Tianjin Univ. MA,2012.
[12] A. H. "Research on capacity optimization of off grid wind," *Application of Energy Technology*, pp. 47-52, 2018.
[13] L. X. Guyayun, "Capacity optimization of grid connected wind solar," *Power Grid and Clean Energy*, vol. 32, pp. :120-126, 2016.
[14] E. A. Strezov, "Assessment of utility energy storage options for increased renewable," *RENEW SUST ENERG REV*, vol. 16, pp. 4141-4147, 2012.
[15] E.N. Nyeche, "Modelling and optimization of a hybrid wind-PV turbine-pumped," *Journal of Cleaner Production*, vol. 250, 2020.
[16] W. L. Weigang, "Optimal allocation of wind water complementary power generation," *Power and Energy*, vol. 35, pp. 88-92, 2014.
[17] J. S. Anagnostopoulos, "Simulation and size optimization of a pumped–storage power plant," *RENEW ENERG*, vol. 33, pp. 1685-1694, 2008.
[18] X. Xu, "Optimized sizing of a standalone PV-wind-hydropower station," *RENW ENERG*, vol. 147 pp.1418-1431, 2020.
[19] Y.Liu, "Optimal sizing of a wind-energy storage system considering," *RENW ENERG*, vol. 147 pp.2470-2483, 2020.
[20] X. L.Gujia, "Optimal allocation of energy storage capacity of wind," Zhejiang Electric Power, vol. 37, pp. 14-17, 2018.
[21] Y. P. Liuyanping, "Capacity optimization and coordinated control method of," Ph.D. dissertation, Dept. Shandong Univ. MA,2014
[22] W. S. Wengshuang, "Danger and opportunity of energy storage," *Management of electric power enterprises in China*, pp. 8-13, 2019.
[23] S. G. Heyi, "The multi-objective capacity optimization of wind-photovoltaic-thermal," *SOL ENERGY*, vol. 195, pp. 138-149, 2020.
[24] R. R. Liu, "The daily and annual technical-economic analysis of the," *SOL ENERGY*, vol. 154, pp. 56-67, 2017.
[25] Y. H. Yanghongtao, "Comprehensive efficiency analysis of Jiangxi," *Hydropower and Pumped Storage*, vol. 5, pp. 78-83, 2019.
[26] Y. Y. Guo, "Operation optimization strategy for wind-concentrated solar power," *ENERG CONVERS MANAGE*, vol. 160, pp. 243-250, 2018.
[27] A.S. Jacob, "Sizing of hybrid energy storage system for a PV based," *APPL ENERG*, vol. 212, pp. 640-653, 2018.
[28] A.M. Abdelshafy, "Optimized energy management strategy for grid," *ENERG*, vol. 192, 2020.
[29] Z. A. Mata, "Techno-economic evaluation of a hybrid," *SOL ENERGY*, vol. 173, pp. 1262-1277, 2018.
[30] D. X. Zhangjianhua, "Capacity optimization of grid connected wind solar energy storage," *Journal of Power System and Automation*, pp. 1-8, 2018.
[31] S. Z. Zeynali, "Two-stage stochastic home energy management," *Sustainable Energy Technologies and Assessments*, vol. 173, 2020.
[32] R. W. Wang, "Multi-objective optimal design of hybrid renewable," *RENW ENERG*, vol. 151 pp.226-237, 2020.
[33] A. R. Rajabi, "A comparative study of clustering techniques for," *RENEW SUST ENERG REV*, vol. 120, 2020.
[34] M. D. Wangbo, "Capacity optimization of independent wind and diesel," *Grid Technology*, vol. 37, pp. 575-581, 2013.
[35] T. C. Chentian, "Research on capacity optimization and photovoltaic maximum," Ph.D. dissertation, Dept. South China University of Technology. MA,2017.
[36] M. S. Matao, "Hybrid pumped hydro and battery storage for," *APPL ENERG*, vol. 257, 2019.
[37] J. J. Roberts, "Robust multi-objective optimization of a renewable based," *APPL ENERG*, vol. 223, pp. 52-58, 2018.
[38] L. Liu, "Multi objective optimization of micro grid based on Pareto," Ph.M. dissertation, Dept. Anhui Univ. MA, 2018.
[39] L.B. Zhang, "Particle swarm optimization for multi-objective," *Computer Research and Development*, pp. 1286-1291, 2004.
[40] "UP77-1500 IIA LT General technical parameters of wind turbine – C", Docin.
[41] "Dongguan Singfo Solar Technology Co., Ltd", ENF website.

Su Guo is an associate professor in School of Energy and Electricity, Hohai University in Nanjing, China. From February 2016 to February 2017, she worked as a visiting scholar at the energy research center of the University of California, San Diego. Now her main research directions are capacity configuration of multi renewable energy combined power generation system and modeling of concentrated solar power generation system

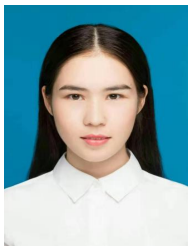

Aynur Kurban is a graduate student in School of Energy and Electricity, Hohai University in Nanjing. She majored in new energy science and Engineering from 2015 to 2019. Her main research direction is capacity optimization of hybrid renewable energy system.

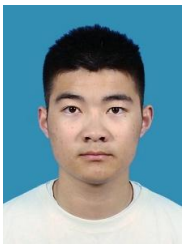

Yi He is a graduate student in School of Energy and Electricity, Hohai University in Nanjing. He majored in fluid machinery. Now his research directions are optimization algorithm, model analysis, capacity optimization of renewable energy system.

Feng Wu is a professor and Dean in College of Energy and Electrical Engineering, Hohai Unviersity in Nanjing. His main research directions are power system modeling and control and modeling and control of renewable energy generation system. He has innovative research results in wave power generation and wind power generation

Huan jin Pei is a graduate student in School of Energy and Electricity, Hohai University in Nanjing. He majored in fluid machinery. Now he mainly studies the operation mechanism and power generation model of concentrated solar power plant

Guotao Song Graduate student of School of energy and electrical engineering, Hohai University, is engaged in research on optimal scheduling of electric thermal integrated energy system. from 2015 to 2019, majored in new energy science and Engineering in Hohai University.